Biosensors and Bioelectronics 62 (2014) 47–51

Contents lists available at ScienceDirect

Biosensors and Bioelectronics

journal homepage: www.elsevier.com/locate/bios

Short communication

Pearl shaped highly sensitive Mn_3O_4 nanocomposite interface for biosensor applications

K. Kamil Reza *, Nawab Singh, Surendra K. Yadav, Manish Kumar Singh [1], A.M. Biradar

Biomedical Instrumentation Section, National Physical Laboratory (CSIR), Dr. K.S. Krishnan Marg, New Delhi 110012, India

ARTICLE INFO

Article history:
Received 27 February 2014
Received in revised form
21 May 2014
Accepted 3 June 2014
Available online 12 June 2014

Keywords:
Mn_3O_4 nanocomposite
Xanthine oxidase
Fish freshness
Electrochemical sensor

ABSTRACT

An electrochemical biosensor based on manganese oxide (Mn_3O_4) and chitosan (Cn) nanocomposite has been fabricated for fish freshness detection. The electrophoretic deposition of Mn_3O_4 nanoparticles (15–20 nm) with Cn has changed their morphological arrangement leading to pearl shaped of Mn_3O_4–Cn nanocomposite on indium tin oxide substrate. Size and morphology of nanocomposite have been confirmed by high resolution transmission electron microscopy (HRTEM), X-ray diffraction (XRD) and scanning electron microscopy (SEM). The results of electrochemical response reveal that this improved sensor has widest detection range of xanthine concentration from 1 to 500 μM and excellent sensitivity of 1.46 μA μM^{-1} cm^{-2}. The fabricated XO_x/Mn_3O_4–Cn/ITO biosensor can detect as low as 1.31 μM of xanthine and lower K_m value of 0.018 μM confirming its superior affinity towards the nanocomposite film.

1. Introduction

The growing demand for fish in the international market has risen considerably in the last decade as large section of human populations living depend on fish industry (Pulvenis et al., 2010). Fish meat freshness is of great importance to food industries for the quality control of fish products. Therefore efforts are going on for estimation of fish freshness by detection of xanthine whose concentrations keep on increasing after the death of fish as a result of metabolic functions. Moreover, xanthine being precursor of uric acid in human body has a clinical significance for kidney related diseases (Berry and Hare, 2003). Thus an efficient device for xanthine detection and quantification is required immediately for clinical analysis as well as fish freshness determination in industry. Xanthine oxidase (XO_x) has been implicated as a key oxidative enzyme by electrochemists for estimation of xanthine (Shan et al., 2009a; Shan et al., 2009b). In this regard, electrochemical detection of xanthine based on nanostructures has been quite successfully reported in literatures (Zhang et al., 2012). Electrochemical sensing has been widely acknowledged as an affordable, rapid, stable, simple and practical technique for a potential miniaturization of devices (Reza et al., 2014, Ali et al., 2014).

In this context, immobilization of xanthine oxidase onto a desired matrix including nanostructured metal oxide (Reza et al., 2013) is considered very important for their high electron mobility, larger surface area for absorption, low detection limit and chemically stable. Apart from that, nano-structured manganese oxide (Mn_3O_4) has shown excellent properties like efficient catalytic activity, high carrier mobility, good biocompatibility, chemical stability and excellent electrochemical properties (Gao et al., 2011). Chitosan (Cn) is a natural cationic biopolymer that has attracted much interest owing to its interesting properties such as inexpensive, stable thin film formation ability and excellent compatibility with biomolecules (Liu et al., 2006). Further, the presence of amino and hydroxyl groups in Cn facilitates in immobilization of enzymes for biosensor application.

Moreover, Cn metal oxide composites are being explored extensively for its excellent sensitivity, high absorption ability, strong enzyme affinity and good stability of the electrodes for clinical investigation of analytes (Kaushik et al., 2009). A very little work based on these materials has been reported in the literature for xanthine sensing (Devi et al., 2012a, 2012b). A combination of Cn and an excellent electrode material like Mn_3O_4 is yet to be attempted for xanthine sensing. We report a fish freshness electrochemical biosensor based on XO_x which was immobilized onto the electrophoretically deposited nanocomposite electrode.

* Corresponding author. Tel./fax: +91 1145609152.
E-mail address: kamilreza@gmail.com (K. Kamil Reza).
[1] Department of Physics, The LNM Institute of Information Technology Jaipur 302031, India.

http://dx.doi.org/10.1016/j.bios.2014.06.013
0956-5663/

2. Experimental

2.1. Reagents and apparatus

All chemicals of analytical grade were purchased from Sigma-Aldrich, India. Mn_3O_4 and its composite have been characterized by using X-ray diffraction (XRD) (Rikagu), high resolution transmission electron microscope (HRTEM, Tecnai G20-stwin), scanning electron microscope (SEM, LEO-440), and Fourier transform infrared spectroscopy (FTIR, PerkinElmer). Electrochemial experiments have been conducted on an Autolab Potentiostat/Galvanostat (Eco Chemie, Netherlands) in phosphate buffer saline (PBS) (50 mM, pH 7.0, 0.9% NaCl) containing 5 mM $[Fe(CN)_6]^{3-/4-}$.

2.2. Fabrication of sensor

Colloidal solution of Mn_3O_4 nanoparticles was synthesized using manganese chloride as the precursor. 100 mM of $MnCl_2$ and 200 mM of NaOH are separately dissolved in 100 ml distilled water and ethanol. Nano-Mn_3O_4 was synthesized by the co-precipitation method by using cetyltrimethylammonium bromide (0.3 mM) as a surfactant (Kavas et al., 2010; Chen et al., 2005). The formed precipitate was washed with de-ionized water and ethanol 10 times and dried at 80 °C for 24 h, and then calcined at 400 °C for 3 h. Further, 20 mg Mn_3O_4 is dispersed in 5 ml of Cn solution prepared by dissolving 1 g Cn powder into 100 ml of 0.1 M acetic acid by constant stirring at room temperature. Then 10 ml solution is used for electrophoretic deposition at 5 V for 100 s onto ITO (area = 0.25 cm^2) glass substrate. Fresh solution of XO_x (0.2 unit/ml) is prepared in PB (50 mM, pH 7.0) and is uniformly spread (10 μL) onto the desired Mn_3O_4–Cn/ITO electrode. The fabricated XO_x/Mn_3O_4–Cn/ITO bioelectrode is stored in a humid chamber for 12 h at room temperature. The bioelectrode was kept at 4 °C for further use. The proposed mechanism for preparation of XO_x/Mn_3O_4–Cn/ITO bioelectrode and immobilization of XO_x onto this electrode is shown in Scheme 1.

3. Results and discussion

3.1. Characterization of biosensor

HRTEM images [Fig. 1(i) and (ii)] show the presence of Mn_3O_4 nanoparticles. The image shows agglomeration due to inter-particle interactions among the nanoparticles. The nanoparticle size range is about 15–20 nm. The inset images of Fig. 1(i) reveal the crystalline nature of the Mn_3O_4 nanoparticles with lattice fringes corresponding to the (211) and (103) planes (JCPDS file 24-0734) respectively. The '*d*' values of lattice fringes belonging to (211) and (103) planes are 0.250 nm and 0.277 nm, respectively. SAED pattern has been shown in the inset of Fig. 1(ii).

SEM [Fig. 1(iii) and (iv)] studies are carried out in order to examine the electrode surface. Mn_3O_4–Cn/ITO electrode reveals formation of spherical nanocomposite structure on to the surface of ITO in Fig. 1(iii). Plenty of white granules (pearl shaped) of Mn_3O_4–Cn nanocomposite were distributed on the ITO substrate. The surface morphology of nanocomposite electrode behaves as an ordered and oriented active surface area providing a friendly microenvironment for XO_x immobilization. The SEM morphology [Fig. 1(iv)] of enzyme immobilized on Mn_3O_4–Cn/ITO electrode shows a well arranged gel like network, which confirms strong enzyme binding. More SEM images are shown in Supplementary data.

The XRD patterns of the synthesized samples are shown in Supplementary Fig. S1(a). The presence of major peaks of Mn_3O_4 nanoparticles with high intensity confirms the high degree of crystallinity as well as purity of the sample. Almost all the diffraction peaks indexed in Fig. S1(a) have been found to be well matched to the tetragonal structure of Mn_3O_4 (JCPDS file 24-0734).

The FTIR spectra of Mn_3O_4–Cn/ITO and XO_x/Mn_3O_4–Cn/ITO electrodes are shown in Fig. S2(b) of Supplementary file. The Mn_3O_4–Cn/ITO electrode (curve i) shows characteristic peaks of Mn–O at 533 cm^{-1}, 585 cm^{-1} and 866 cm^{-1}. The characteristic peaks at 3424 cm^{-1}, 1561 cm^{-1} and 1263 cm^{-1} are due to O–H, N–H and CH_2 absorption bands of Cn respectively. Further, Mn_3O_4–Cn/ITO electrode shows peaks at 1650 cm^{-1} of N–H band of amines and 1074 cm^{-1} of C–N stretching of amines. Curve (ii)

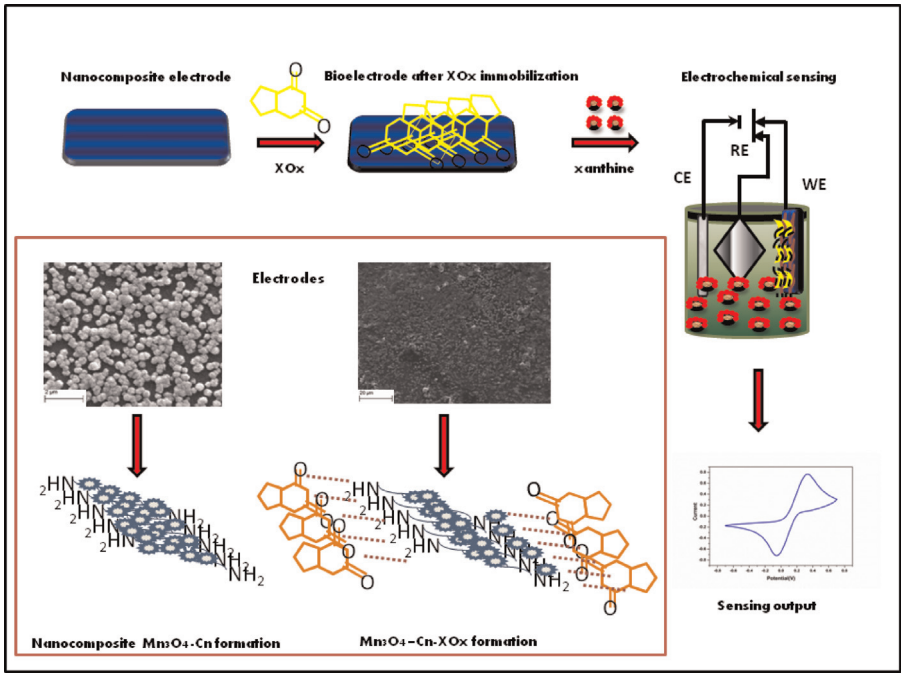

Scheme 1. Mn_3O_4 nanocomposite based biosensor for fish freshness detection.

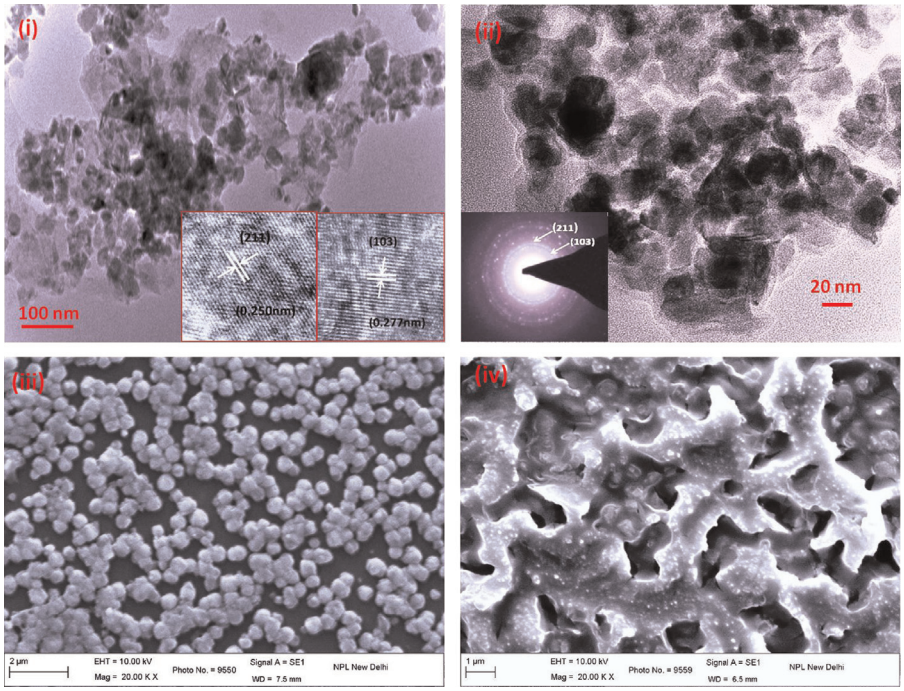

Fig. 1. (i) HRTEM images of Mn_3O_4 nanoparticle and inset shows '*d*' values of 211 and 103 lattice planes, (ii) high resolution image of Mn_3O_4 nanoparticles, (iii) SEM images of Mn_3O_4–Cn/ITO electrode and (iv) XO_x/Mn_3O_4–Cn/ITO bioelectrode after XO_x immobilization.

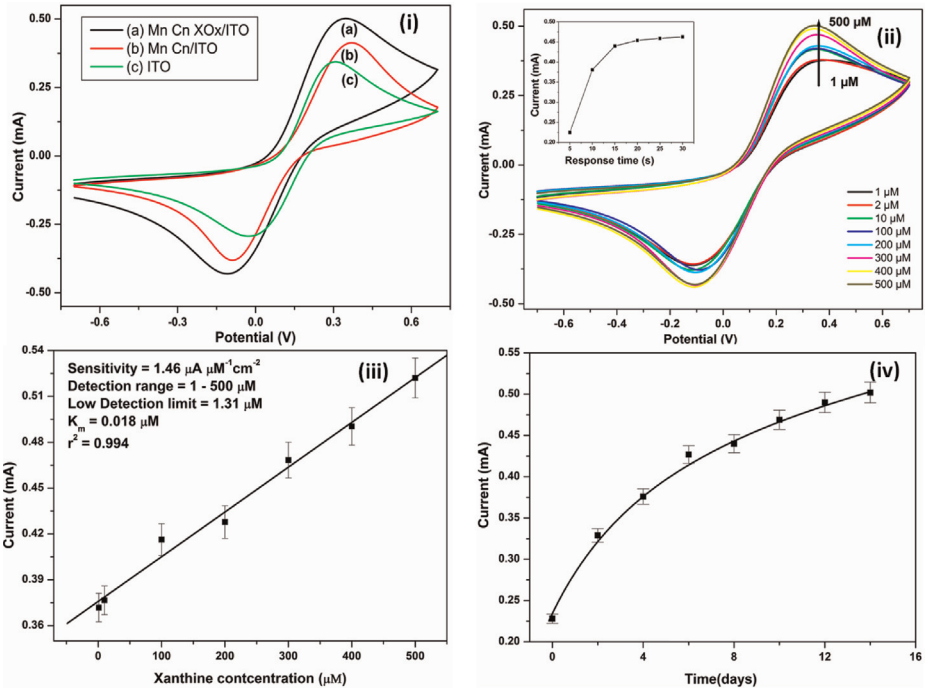

Fig. 2. (i) The CV of (a) the XO_x/Mn_3O_4–Cn/ITO bioelectrode, (b) Mn_3O_4–Cn/ITO electrode and (c) ITO electrode in PBS. (ii) The CV of the XO_x/Mn_3O_4–Cn/ITO bioelectrode as a function of xanthine concentration (1–500 µM) in PBS and inset shows response time studies. (iii) Calibration curve between amperometric current response and xanthine concentration during sensing. (iv) Real sample study of the fabricated sensor.

shows peaks at 1694 cm^{-1}, 1373 cm^{-1}, 1320 cm^{-1}, 1150 cm^{-1} and 1032 cm^{-1} after immobilization of XO_x onto Mn_3O_4–Cn/ITO electrode. The 1032 cm^{-1} peak corresponds to C–N stretch and 1694 cm^{-1} belongs to C=O stretching of amide carbonyl in XO_x.

The Cyclic Voltammetry (CV) studies of Mn_3O_4–Cn/ITO electrode shows high magnitude of current of 0.413 mA (curve b) as compared to that of bare ITO (0.343 mA, curve c), shown in Fig. 2 (i). This may be due to well arranged spherical nanostructures of the Mn_3O_4 and Cn nanocomposite which provide increased electro-active surface area resulting in enhanced redox current. However, after immobilization of XO_x onto Mn_3O_4–Cn/ITO electrode, the magnitude of current value of XO_x/Mn_3O_4–Cn/ITO (curve a) electrode increases to 0.501 mA indicating a strong binding of XO_x with the electrode that perhaps helps in transport of charge carriers resulting in fast electron communication between the matrix and XO_x molecules. This indicates that a larger surface area of nanocomposite facilitates higher mass diffusion efficiency due to electrochemical activation of enzymes active site

resulting in enhanced redox current (Ali et al., 2013). The higher activity of XO_x/Mn_3O_4–Cn/ITO bioelectrode obtained at pH 7.0 reveals that bioelectrode is more active at pH 7.0 (data not shown).

The CV studies have been carried out on XO_x/Mn_3O_4–Cn/ITO bioelectrode as a function of scan rate varying from 10 to 120 mV/s (Supplementary Fig. S3). It can be seen that both anodic (i_a) and cathodic (i_c) peak currents of the electrode increase linearly and are proportional to the scan rate indicating the diffusion controlled electron transfer process (inset of Fig. S3).

The diffusion coefficient (D) of the redox group of XO_x/Mn_3O_4–Cn /ITO bioelectrode has been calculated using the Randel–Sevcik equation:

where I_p is peak current (A), n is electron stoichiometry, A is electrode area (0.25 cm^2), D is diffusion coefficient, C is concentration of redox species (5×10^{-6} mol/cm^3) and υ is scan rate. The diffusion coefficient found out to be 1.631×10^{-7} cm^2/s.

3.2. Electrochemical response of the biosensor

Electrochemical response studies of XO_x/Mn_3O_4–Cn/ITO bioelectrode have been carried out as a function of xanthine concentration in the presence of 100 μl xanthine solution using CV of 50 mM PBS (pH 7, 0.9% NaCl) containing 5 mM $[Fe(CN)_6]^{3-/4-}$. It was observed that the magnitude of current obtained for the XO_x/Mn_3O_4–Cn/ITO bioelectrode gradually increases on addition of xanthine concentration in Fig. 2(ii). The added concentration of xanthine produces more H_2O_2 which further produces more electrons resulting in increased currents. This enhancement of electrochemical current response may be due to well-arranged and homogenous network of bio-interface of the Mn_3O_4–Cn nanocomposite electrode that provide good path for transport of electrons generated during oxidation of xanthine that are transferred to electrode via manganese ion (Singh et al., 2011). Also, the presence of pearl shaped morphology of Mn_3O_4–Cn/ITO electrode results in improved electronic and ionic transport due to uniformly distributed Mn_3O_4–Cn nanocomposite rather than clustered matrix resulting in a three-dimensional electron conductive network (Kaushik et al., 2009). Further, the response time of the XO_x/Mn_3O_4–Cn/ITO bioelectrode was found to be about 15 s which is attributed to faster electron communication feature of Mn_3O_4–Cn nanocomposite [inset of Fig. 2(ii)].

Fig. 2(iii) shows good linearity in the calibration curve with concentration range of 1–500 μM and the current varies linearly with xanthine concentration (μM) with correlation coefficient of 0.994. The sensitivity of the XO_x/Mn_3O_4–Cn/ITO bioelectrode calculated from the slope of curve has been found to be 1.46 μA μM^{-1} cm^{-2}. The high value of sensing may be attributed to high surface to volume ratio of nanocomposite with better transportation of electron along the film surface. The low detection limit is found to be 1.31 μM.

The Michaelis–Menten constant (K_m) of 0.018 μM using the Hanes plot indicates high affinity of enzyme towards the electrode due to favorable orientation of XO_x and higher loading of XO_x provided by the Mn_3O_4–Cn/ITO thin film surface (Fig. S4 of Supplementary file). The stability of the XO_x/Mn_3O_4–Cn/ITO bioelectrode has been studied by measuring the amperometric response at a xanthine concentration of 100 μM cm^2 over a period of 8 weeks (Fig. S5 of Supplementary file). The XO_x/Mn_3O_4–Cn/ITO bioelectrode has been used daily. The response of bioelectrode almost remains the same up to 5 weeks and after that it decreases to approximately 30% of the initial response after 8 weeks. This shows good stability of the fabricated sensor.

The selectivity of the XO_x/Mn_3O_4–Cn/ITO bioelectrode has been assessed in the presence of other analytes such as glucose (5 mM), cholesterol (5 mM), uric acid (0.5 mM) and lactic acid (0.5 mM) (Fig. S6 of Supplementary data). This bioelectrode prevents the diffusion of glucose, cholesterol, and lactic acid to the electrode. It has been found that the XO_x/Mn_3O_4–Cn/ITO electrode responds to uric acid indicating that anodic detection of xanthine suffers from the interference of uric acid. Our bioelectrode shows excellant reproducibility for xanthine concentrations of 300 μM with low relative standard deviations (RSD) (1.69%, $n=5$), proving its good accuracy. Table I shows the calculation details (shown in Fig. S7 and Table I of Supplementary file).

The real sample analysis of xanthine detection has been conducted in fresh water fish sample. The chopped fish of about 5 g is made into fine paste in the presence of $HClO_4$ and NaOH for precipitation of protein. Then it is mechanically stirred, centrifuged and its pH adjusted to 7.0. Now xanthine is determined using XO_x/Mn_3O_4–Cn/ITO working electrode and experiment is continued every 2 days for 2 weeks to study the real sample. The steady increase in xanthine concentration as a function of days can be seen in Fig. 2(iv).

The XO_x/Mn_3O_4–Cn/ITO bioelectrode showed improved sensitivity and wider linearity for xanthine detection with longer stability than other biosensors reported calcium carbonate (Shan et al., 2009a), Au/carbon nanohorn (Zhang et al., 2012), ZnO-NP/CHIT/c-MWCNT/PANI (Devi et al., 2012a) and Zinc oxide-PPy (Devi and Yadav, 2011) based electrodes. This may be due to the presence of large active surface area with spherical morphology of the electrode which enhances the sensing parameters for xanthine detection. We have reported a good response time of 15 s which is slower than reported by Devi et al. (2012a) of 4 s, Shan et al. (2009b) of 8 s but faster than Devi et al. (2012b) of 35 s and Dodevska et al. (2010) of 60 s. This electrode shows excellent stability of 60 days better than that of Zhang et al. (2012) of 14 days, Devi et al. (2012b) of 15 days, Devi et al. (2012a) of 30 days, but less than that of Devi et al. (2011) having 100 days of stability. Further, lower K_m value (0.018 μM) of this sensor is better than those reported in literatures mentioned above. We have summarized the sensing parameters in Table II (Supporting information) which shows the characteristics of this sensor along with those reported in the literatures. This fabricated biosensor provides a sensitive, efficient, simple, low cost electrochemical sensing technique for xanthine monitoring.

4. Conclusions

It has been demonstrated that Mn_3O_4–Cn nanocomposite has been used successfully for xanthine detection by the electrochemical method. This nanocomposite film provides a better matrix with improved sensitivity of 1.46 μA μM^{-1} cm^{-2}, longer stabilty of 60 days and faster electrochemical response (15 s) towards the xanthine detection. This biosensor exhibits lower K_m value 0.018 μM with linear regression at 0.994 and wide linear range of 1–500 μM. The enhanced electrochemical parameters of the fabricated sensor may result from the presence of spherical pearl shaped nanostructure. The detection limit of this biosensor is 1.31 μM which can be improved further. We have investigated the real sample for measurement of xanthine concentration to demonstrate the practical application of sensor in fish fressness. Therefore, it may be interesting to utilize this electrode for fabrication of biosensors in food freshness, food pathogens, food toxins detection and point of care dignostics.

Acknowledgments

We thank Director, National Physical Laboratory, New Delhi, India for providing the facilities. K. Kamil reza thanks Prof. B.D. Malhotra, Dr. V.V. Agrawal and Dr. G. Sumana for their constant guide and support. Thanks are due to all lab members for their well wishes. The financial support received under Department of Science and Technology projects (GAP-081132) is gratefully acknowledged.

Appendix A. Supplementary information

Supplementary data associated with this article can be found in the online version at http://dx.doi.org/10.1016/j.bios.2014.06.013.

References

Ali, M.A., Solanki, P.R., Patel, M.K., Dhayani, H., Agrawal, V.V., John, R., Malhotra, B.D., 2013. Nanoscale 5, 2883.
Ali, M.A., Reza, K.K., Srivastava, S., Agrawal, V.V., John, R., Malhotra, B.D., 2014. Langmuir 30, 4192–4201.
Berry, C.E., Hare, J.M., 2003. J. Physiol. 555, 589–606.
Chen, Z.W., Lai, J.K.L., Shek, C.H., 2005. Appl. Phys. Lett. 86, 181911.
Devi, R., Yadav, S., Pundir, C.S., 2011. Biosens. Bioelectron. 26, 3420–3426.
Devi, R., Yadav, S., Pundir, C.S., 2012a. Analyst 137, 754.
Devi, R., Narang, J., Yadav, S., Pundir, C.S., 2012b. J. Anal. Chem. 67, 273–277.
Dodevska, T., Horozova, E., Dimcheva, N., 2010. Cent. Eur. J. Chem. 8, 19.
Gao, J., Lowe, M.A., Abruña, H.D., 2011. Chem. Mater. 23, 3223–3227.
Kaushik, A., Solanki, P.R., Pandey, M.K., Ahmad, S., Malhotra, B.D., 2009. Appl. Phys. Lett. 95, 173703.
Kavas, H., Durmus, Z., Senel, M., Kazan, S., Baykal, A., Toprak, M.S., 2010. Polyhedron 29, 1375–1380.
Liu, Y., Qu, X., Guo, H., Chen, H., Liu, B., Dong, S., 2006. Biosens. Bioelectron. 21, 2195–2201.
Pulvenis, J.F., Seligny, D., Grainger, R., Gumy,A., Wijkstrom, U., The State of World Fisheries and Aquaculture (U.S. FAO Fisheries and Aquaculture Department, Rome, 2010).
Reza, K.K., Singh, M.K., Yadav, S.K., Singh, J., Agrawal, V.V., Malhotra, B.D., 2013. Sens. Actuators B Chem. 177, 627–633.
Reza, K.K., Srivastava, S., Yadav, S.K., Biradar, A.M., 2014. Mat. Lett. 126, 126–130.
Shan, D., Wang, Y., Xue, H., Cosnier, S., 2009a. Sens. Actuators B Chem. 136, 510–515.
Shan, D., Wang, Y., Zhu, M., Xue, H., Cosnier, S., Wang, C., 2009b. Biosens. Bioelectron. 24, 1171–1176.
Singh, J., Kalita, P., Singh, M.K., Malhotra, B.D., 2011. Appl. Phys. Lett. 98, 123702.
Zhang, L., Lei, J., Zhang, J., Ding, L., Ju, H., 2012. Analyst 137, 3126.